AIRS MEDICAL

AI-Powered MR image enhancement solution SwiftMR™

Clinical Implications and Use Cases

Kevin (Seungwook) Yang, Ph.D, Head of Clinical Research
Sohyun Kim, Clinical Research Scientist
Minju Cho, Clinical Research Scientist
Geunu Jeong, MD, Head of SwiftMR Research & Development
Kyungeun Jang, Ph.D, Research Scientist

Hurdles in clinical MR imaging

Magnetic resonance imaging (MRI) is a non-invasive diagnostic exam that does not use ionizing radiation and that enables structural, volumetric, and functional imaging with excellent soft tissue contrast. Despite its importance in modern medical practice, long scan times for acquiring diagnostic-quality images remain a challenge. Much of the related scientific research and technological development efforts over the past decades have been focused on addressing this issue. As a result, acceleration techniques such as parallel imaging and compressed sensing have rapidly become part of clinical routine.

Even so, scan time remains one of the major hurdles preventing the more ubiquitous use of MRI across different clinical scenarios. Signal-to-noise ratio (SNR), spatial resolution, contrast, and the amount of artifacts seen on the image are all related to scan time, which healthcare professionals struggle to balance in different clinical situations. This inherent trade-off between scan time and image quality forces radiology professionals to compromise depending on the patient, their clinical needs, and the preferences of the referring clinician, potentially affecting diagnostic confidence and accuracy. Additionally, increasing demands for advanced imaging lead to operational inefficiencies for healthcare institutions and delayed care delivery for patients – in some cases by more than two weeks(1,2). Studies have shown that this directly translates to patient dissatisfaction(3), underscoring the need for better management of patient queues both off- and on-site(4). From the patients' perspective, anxiety and physical discomfort during the exams significantly impact not only their satisfaction with the procedure, but also the clinical outcomes (5–8).

MR image reconstruction in the age of AI: SwiftMR™

With the advent of artificial intelligence (AI), image quality enhancement and scan time reduction may be achieved simultaneously. This is made possible by a process called deep learning (DL), in which an AI algorithm is trained using millions of MR data to perform a specific task – in this case noise reduction and spatial resolution enhancement. What makes SwiftMR™, a DL-based MR image reconstruction software developed by AIRS Medical, unique is that it performs image enhancement in the Digital Imaging and Communications in Medicine (DICOM) domain instead of in the raw data or k-space. Contextual information related to the image acquisition is pulled from the input DICOM image, enabling physics-informed denoising and resolution enhancement. This enables SwiftMR™ to show robust performance in diverse clinical applications in a hardware-agnostic (e.g., scanner vendor, field strength) and image-agnostic (e.g., pulse sequence, anatomy, image type) manner. Another unique feature of SwiftMR™ is its highly-customizable performance in noise reduction and resolution enhancement, ensuring tailored implementation depending on the clinical needs of the radiology practitioners. An example of this user-selectable feature is illustrated in Figure 1. Detailed technical information can be found in our published work by Jeong, et al (9). SwiftMR™ is being marketed in 19 countries including the United States (FDA 510(k) clearance) and the European Union (MDR CE mark).

With a disruptive innovation such as SwiftMR™, extensive clinical validation and continued technological improvement are key to ensuring its clinical translation. In addition to numerous ongoing studies and existing peer-reviewed

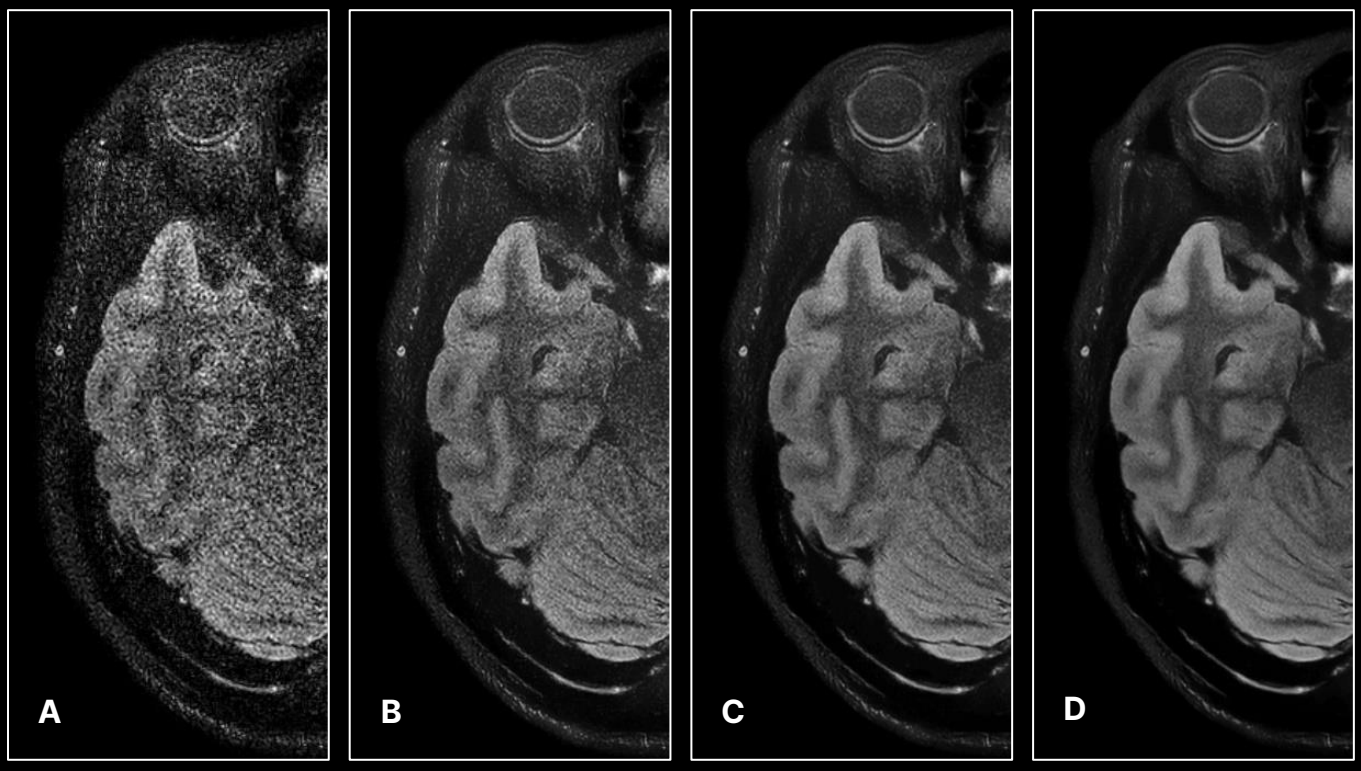

Figure 1 - Example of customizable denoising levels by SwiftMR™ is illustrated with representative images from select denoising levels. (A) Highly-accelerated input (original) image along with SwiftMR™-processed images at: (B) denoising level “2”, (C) denoising level “4”, and (D) denoising level “6”. Notice the reduction in noise and improvement in image clarity as the denoising level increases.

publications utilizing SwiftMR™, this clinical whitepaper aims to provide a brief overview of its vetting process by 18 board-certified radiologists from six different radiology subspecialties

The validation process

Study dataset

A large-scale, multi-center, multi-reader study involving various radiology subsections was conducted, comparing accelerated images processed with SwiftMR™ to the standard-of-care (SOC). A detailed breakdown of the dataset collected for this validation study is presented below in Table 1. Note that exams may consist of multiple images depending on the clinical scenario, in which clinically routine images such as T1, T2, T2*, PD, FLAIR, DWI, MRA were included in the comparison.

Study Methods and Statistical Analysis

Three board-certified radiologists from each of the six different subspecialties – neuro, musculoskeletal, cardiovascular, breast, abdomen, and genitourinary – were recruited for this validation study. Experience levels ranged from 5-24 years in practice following board certification, with a mean of 12.3 years of experience.

Table 1 - Study dataset breakdown

Category	Number of exams
Total number of exams	184
Demographics	
By anatomical localization	
Neuro – brain, head & neck, spine	36
Musculoskeletal – shoulder, wrist, hip, knee, ankle	89
Body – cardiac, breast, abdomen, pelvis (GU)	59
By existence of pathologies	
With confirmed pathology	80
Without confirmed pathology	104
By technical parameter	
Field strength	
0.25T	22
1.5T	81
3.0T	81
By MR manufacturer	
GE Healthcare	32
Philips	53
Siemens Healthineers	77
Esaote	22

Participating radiologists were sequentially presented with a single randomized series of DICOM images per session and were blinded to the type of image presented and the presence of findings or pathologies. The radiologists were then asked to individually grade the conspicuity of normal anatomical structures and lesions (if any) along with overall image quality in terms of perceived signal-to-noise ratio (SNR), image sharpness, and contrast.

Images were viewed on diagnostic radiology monitors used in the participating radiologists' routine clinical practice, and evaluations were based on a Likert scale metric as follows: 1-non-diagnostic, 2-limited diagnostic capability, 3-fair with significant room for improvement, 4-good with few minor insufficiencies, 5-excellent with no limitation in interpretation. For statistical analysis, paired *t*-tests were performed for SwiftMR™ versus SOC and SwiftMR™ versus accelerated image comparisons; *p*-values < 0.05 were considered statistically significant.

Findings

Overall subjective scores

The results were analyzed first by counting the number of instances where SwiftMR™-processed accelerated images received higher, equal, or lower scores than the SOC. In 74.7% of cases, SwiftMR™-processed images were scored higher than the SOC; 19.0% were scored the same as the SOC; and 6.3% scored lower. A visual representation of the results is shown in Figure 2.

The averaged subjective scores from all images showed that the SwiftMR™-processed accelerated images received the highest scores across all evaluation categories, with noticeable differences observed in subjective SNR and resolution categories. A summary is given in Figure 3.

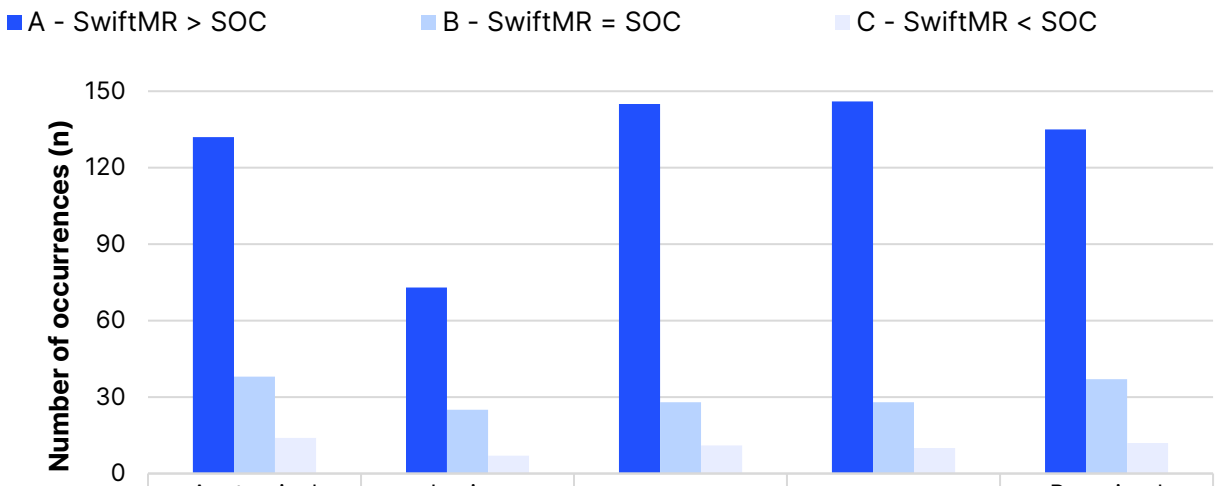

	Anatomical Conspicuity	Lesion Conspicuity	Perceived SNR	Resolution	Perceived Contrast
A - SwiftMR > SOC	132	73	145	146	135
B - SwiftMR = SOC	38	25	28	28	37
C - SwiftMR < SOC	14	7	11	10	12

Figure 2 - Bar graphs showing the number of occurrences for each rankings. A (blue): score of SwiftMR™-processed accelerated image > SOC, B (green): score of SwiftMR™-processed accelerated image = SOC, C (grey): score of SwiftMR™-processed accelerated image < SOC.

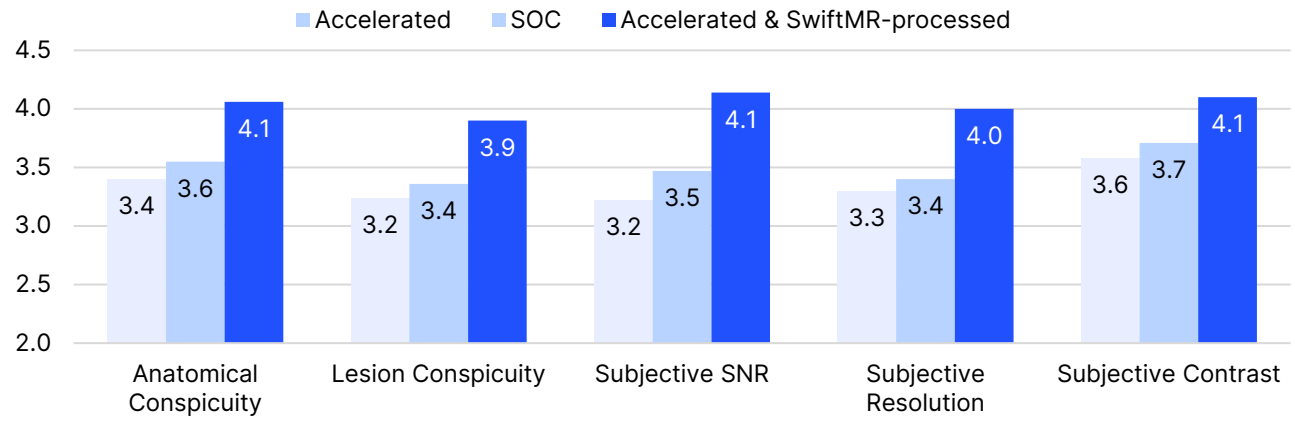

Figure 3 - Average subjective scores from all readings per evaluation category. *P-value for comparison between the SOC MRI versus SwiftMR™-processed accelerated MRI. †P-value for comparison between the accelerated MRI versus SwiftMR™-processed accelerated MRI. All p-values were less than 0.001.

In the following sections, subgroup evaluation results and sample images representing SwiftMR™'s effect in different anatomical locations and imaging sequences will be illustrated.

Subgroup results & examples – Neuro (brain & spine)

The averaged scores for brain and spine images showed that SwiftMR™-processed images exhibited superior quality when compared with both the accelerated input images and the SOC, with the largest differences observed in subjective SNR and resolution. The results are summarized in Table 2.

Subgroup analysis – Musculoskeletal (shoulder, wrist, hip, knee, ankle)

In musculoskeletal imaging, SwiftMR™-processed images likewise exhibited superior quality compared with the SOC and accelerated input images. Larger differences were seen across all evaluation categories when compared with the neuro subgroup, with noticeable differences detected for anatomical conspicuity, SNR, and spatial resolution. Evaluation results are summarized in Table 3.

Subgroup analysis – Body (breast, cardiac, abdomen, genitourinary)

In body imaging, SwiftMR™-processed images showed higher scores compared with the SOC

Table 2 - Averaged scores for neuro subgroups.

	Accelerated	SOC	SwiftMR™ -processed	p-value*	p-value†
Anatomical Conspicuity	3.31	3.63	4.11	< 0.001	< 0.001
Lesion Conspicuity	3.10	3.46	4.00	< 0.001	< 0.001
Subjective SNR	2.98	3.44	4.09	< 0.001	< 0.001
Subjective Resolution	3.19	3.47	4.03	< 0.001	< 0.001
Subjective Contrast	3.37	3.71	4.18	< 0.001	< 0.001

*p-value comparing accelerated input image and SwiftMR™-processed accelerated image, †p-value comparing standard-of-care image and SwiftMR™-processed accelerated image.

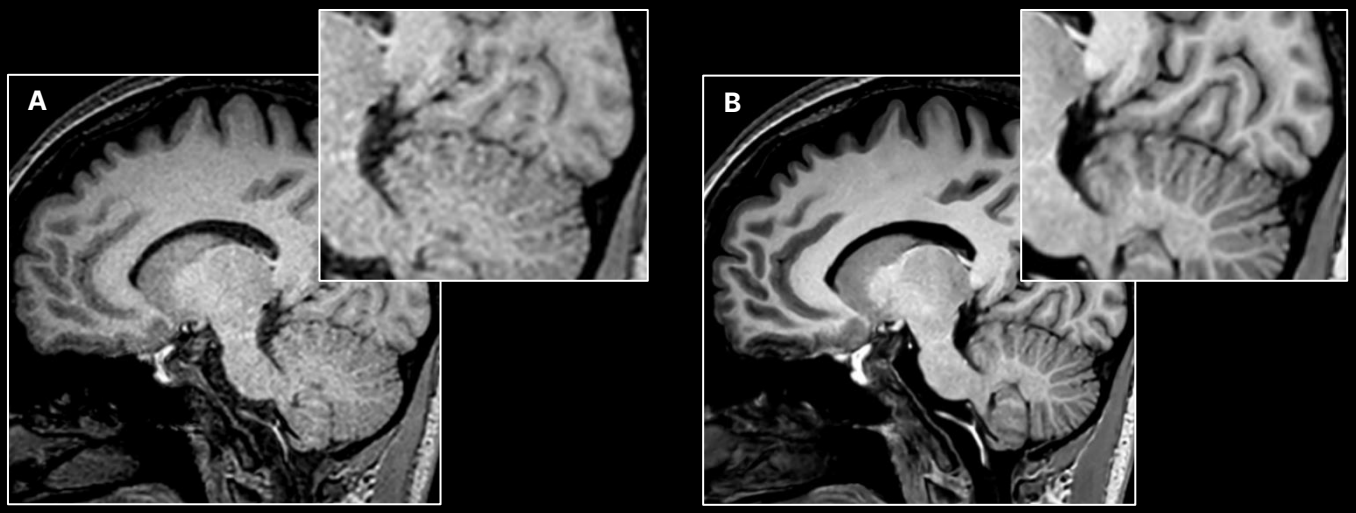

Figure 4 - SNR improvement example with SwiftMR for 3D T1-weighted imaging. (A) SOC image at 1.0 x 1.0 x 1.0 mm and (B) Same subject scanned under optimized parameters for improving image contrast in same scan time. Note the considerable improvement in SNR and spatial resolution after applying SwiftMR, particularly in the highlighted regions.

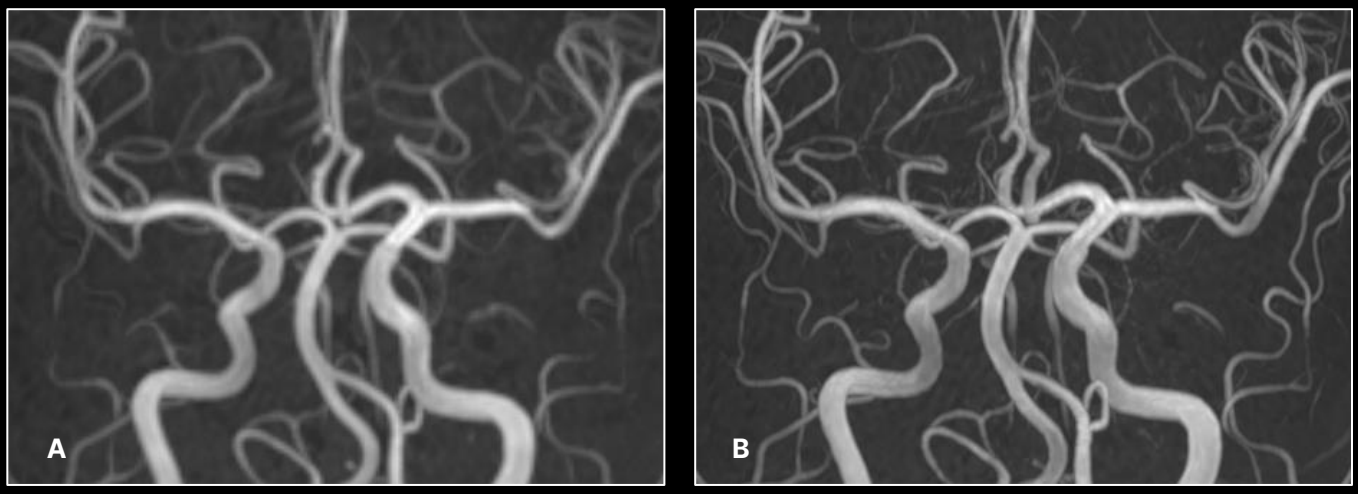

Figure 5 - Example of spatial resolution improvement with SwiftMR for 3D Time-of-Flight (TOF) MRA. (A) SOC image at 0.6 x 0.8 x 1.2 mm and (B) 64% accelerated scan at 0.6 x 0.8 x 1.2 mm processed with SwiftMR. Structural conspicuity of major arteries and peripheral branches has dramatically increased after SwiftMR reconstruction.

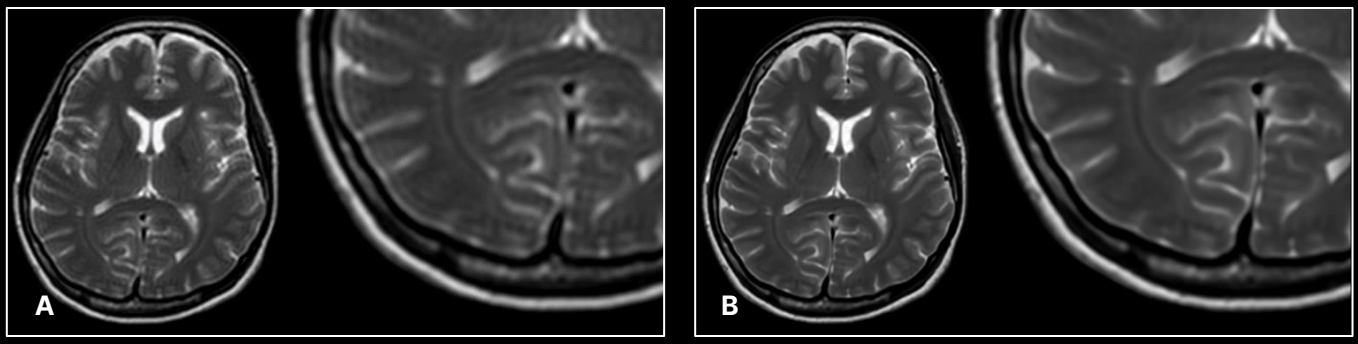

Figure 6 - Example of truncation artifact improvement with SwiftMR. (A) A low-resolution image acquired at 1.6 x 1.6 x 4.0 mm to exaggerate truncation artifacts (B) Same image processed with SwiftMR. Note the considerable improvement in spatial resolution and significant removal of truncation artifacts observed across the image.

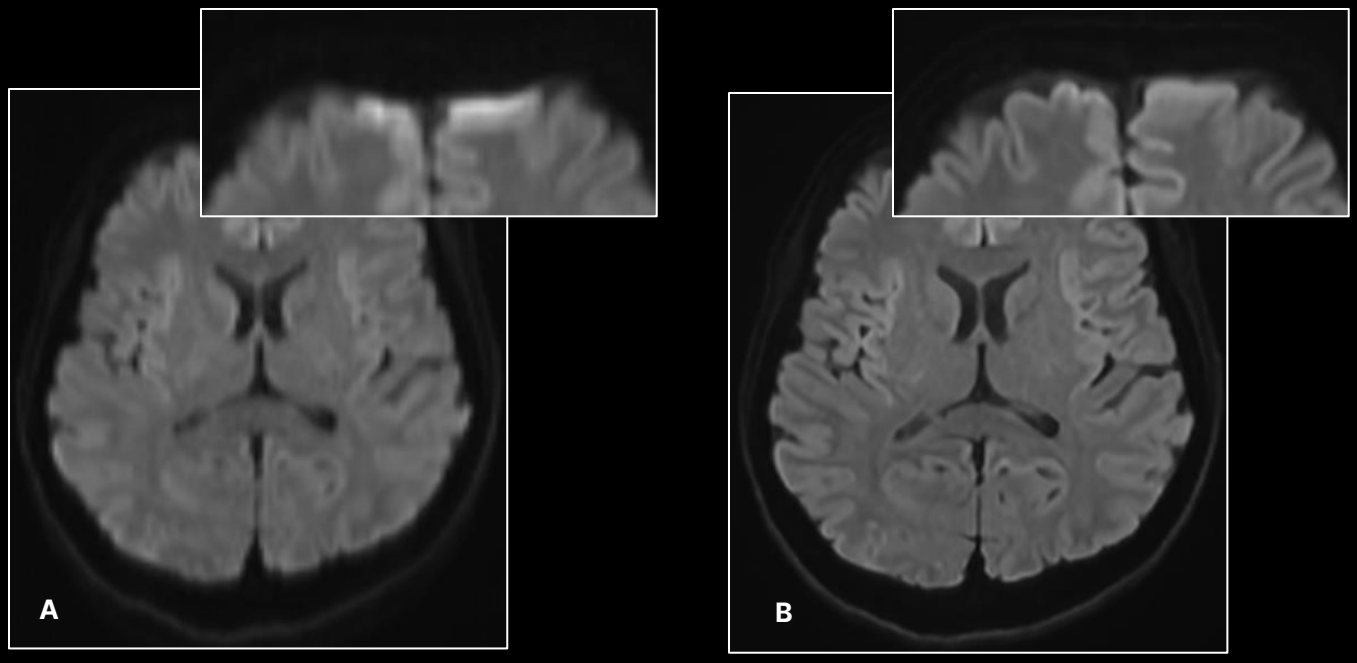

Figure 7. Example of distortion artifact correction by SwiftMR reconstruction combined with optimized imaging protocol for diffusion weighted imaging. (A) SOC image at 1.5 x 1.9 x 3.0 mm and (B) SwiftMR-reconstructed image from an optimized input at same scan time. Spatial resolution has increased, along with noticeable improvement of the geometric distortion artifact in the frontal lobe.

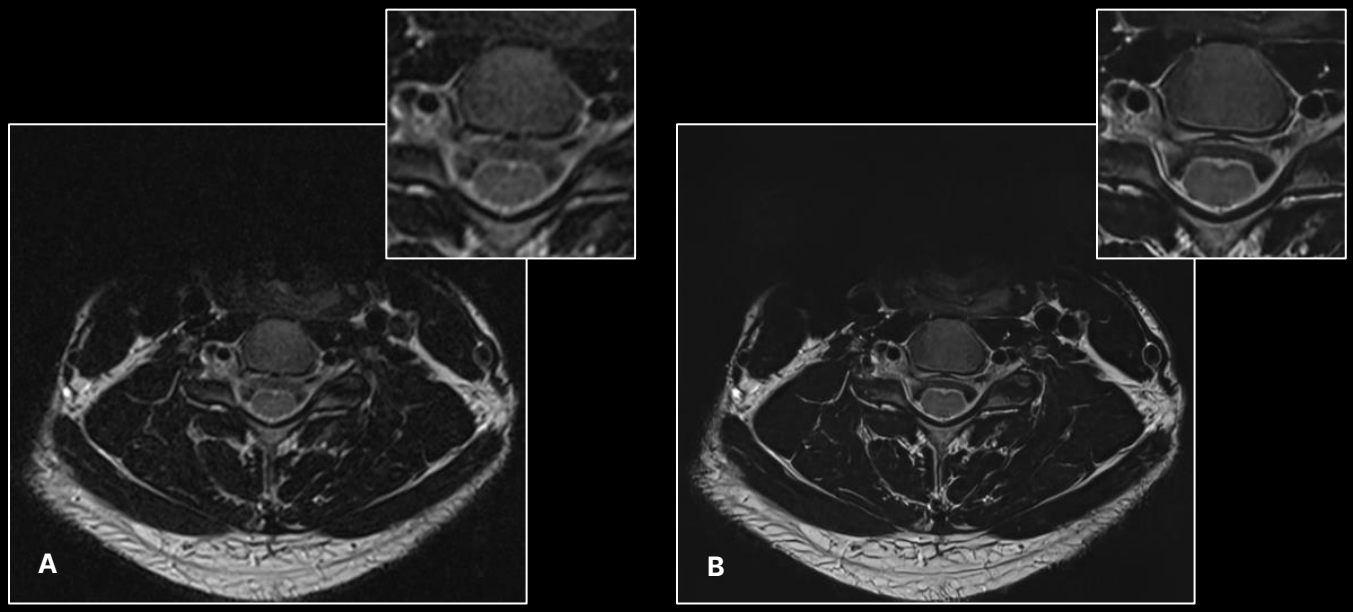

Figure 8. Example of noise reduction and resolution enhancement with SwiftMR for T2-weighted cervical spine MRI. (A) SOC image at 0.7 x 0.7 x 3.0 mm and (B) 34% faster scan processed with SwiftMR. SNR and spatial resolution has noticeably increased.

Table 3 - Averaged scores for musculoskeletal subgroups.

	Accelerated	SOC	SwiftMR™ -processed	p-value*	p-value†
Anatomical Conspicuity	3.09	3.27	3.98	< 0.001	< 0.001
Lesion Conspicuity	3.26	3.46	3.99	< 0.001	< 0.001
Subjective SNR	2.89	3.18	4.11	< 0.001	< 0.001
Subjective Resolution	2.97	3.10	3.91	< 0.001	< 0.001
Subjective Contrast	3.36	3.51	3.97	< 0.001	< 0.001

*p-value comparing accelerated input image and SwiftMR™-processed accelerated image, †p-value comparing standard-of-care image and SwiftMR™-processed accelerated image.

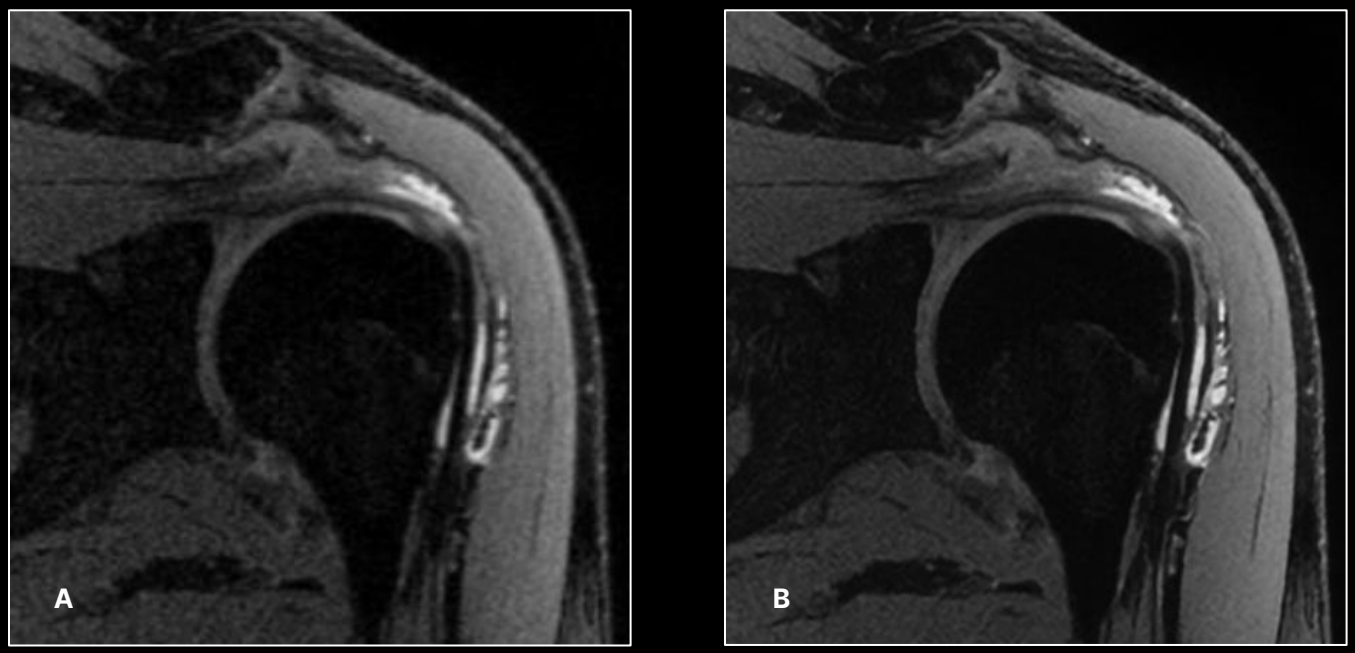

Figure 9 - Denoising & resolution enhancement example for 3D T2*-weighted imaging of the shoulder. (A) SOC image at 0.6 x 0.7 x 0.6 mm, (B) SwiftMR-processed SOC image. Significant reduction in noise across the image and in-plane resolution can be seen.

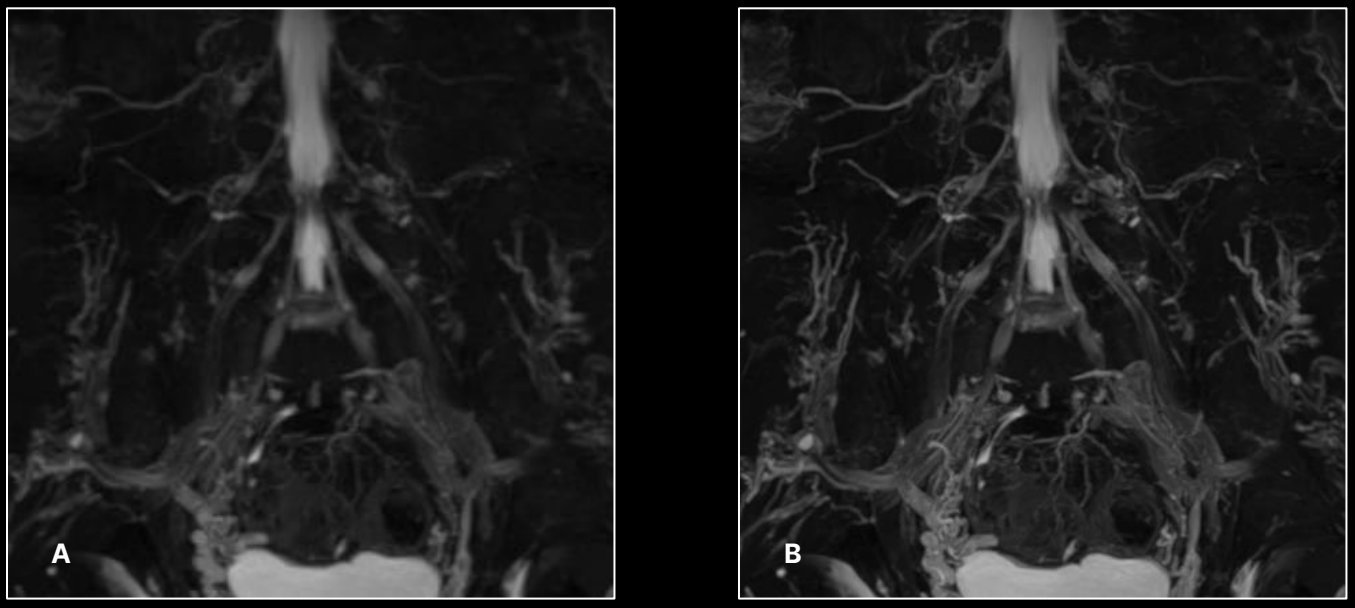

Figure 10 - Resolution enhancement example for a lumbosacral plexus neurography. (A) SOC image at 1.1 x 1.4 x 1.4 mm with MIP thickness of 20.0mm, (B) SwiftMR-processed SOC image. Significant spatial resolution enhancement can be observed from the reconstructed image.

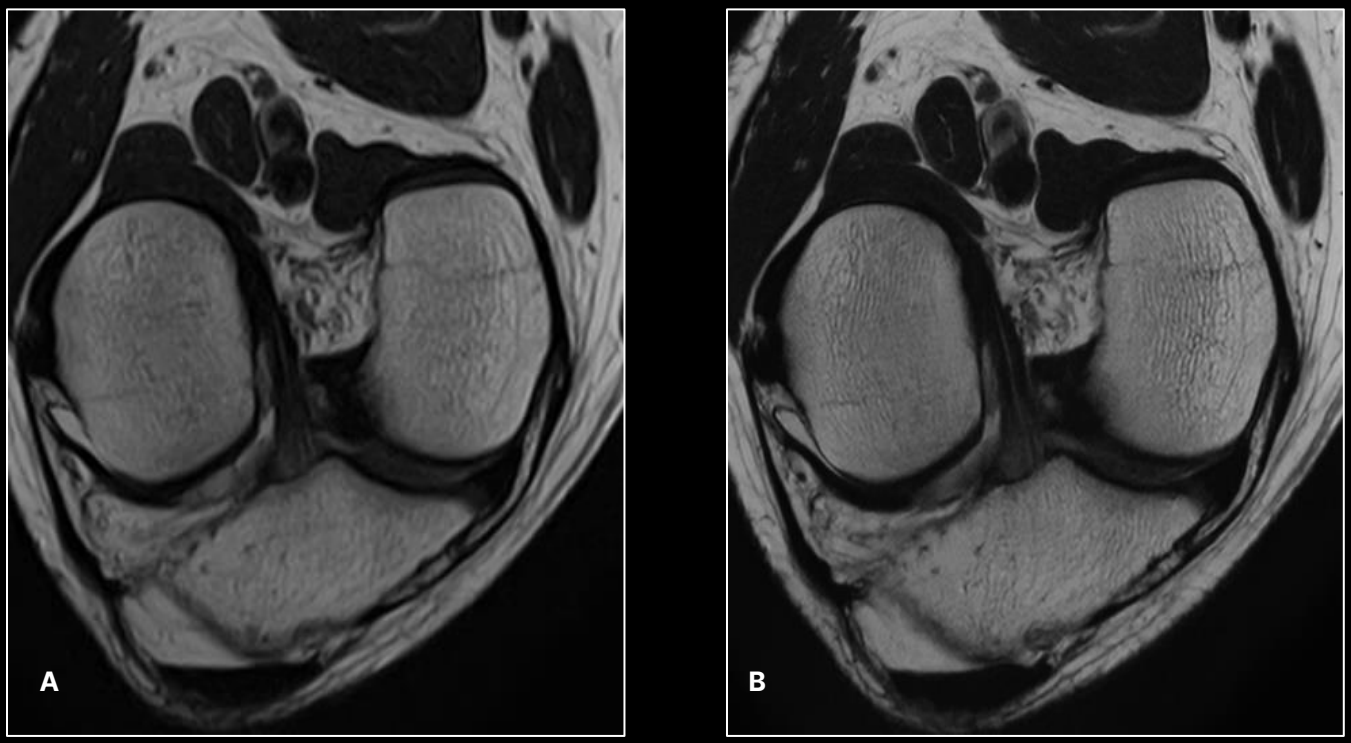

Figure 11 - Resolution enhancement example for 2D T2-weighted imaging of the knee. (A) SOC image at 0.5 x 0.7 x 2.0 mm, (B) 40% faster scan at same acquisition voxel size & slice thickness processed with SwiftMR. Significant increase in spatial resolution can be seen in the results, especially for the trabecular structures of the distal femur.

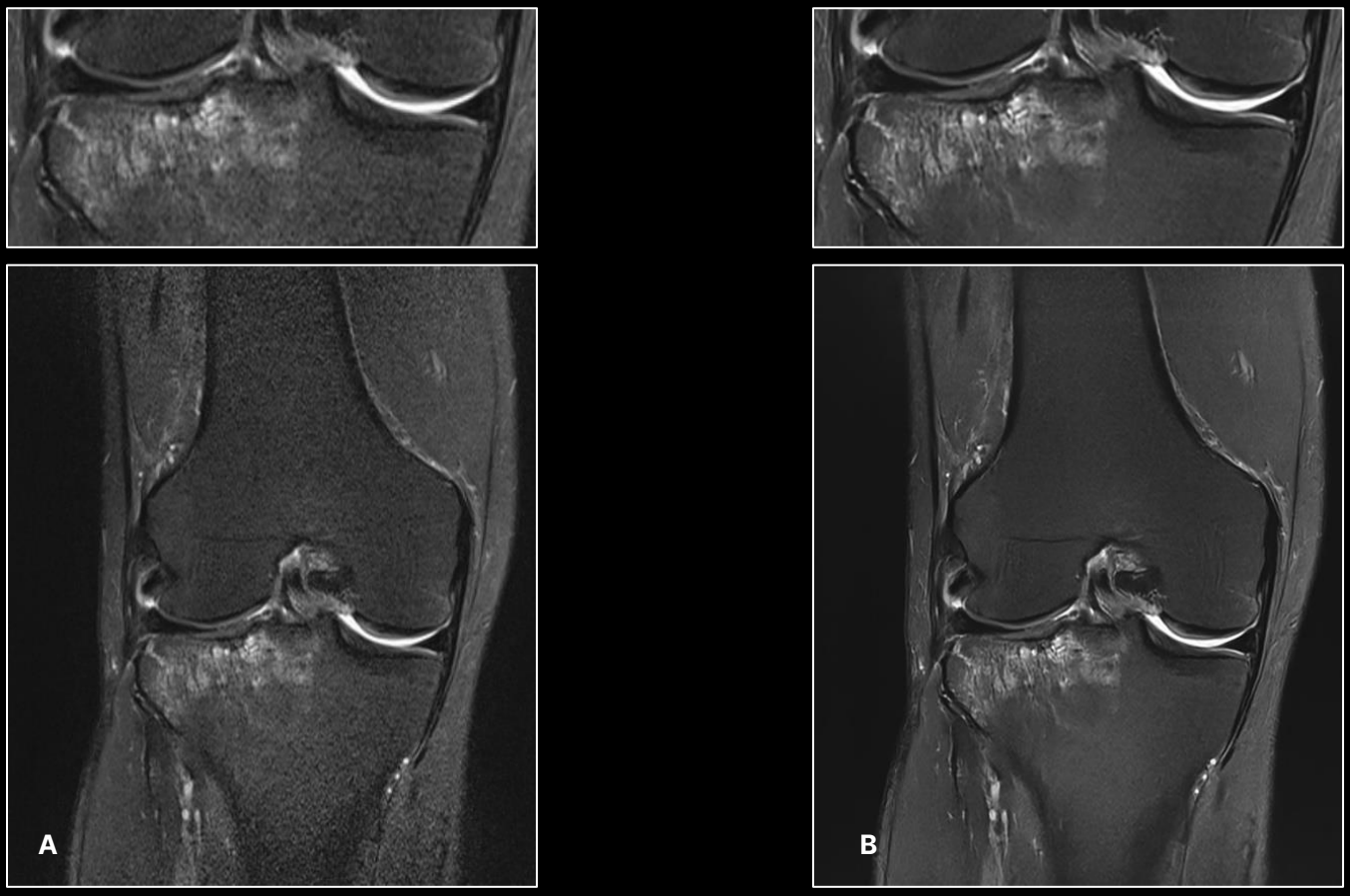

Figure 12. Denoising and resolution enhancement example for 2D fat-saturated T2-weighted imaging of the knee. (A) SOC image at 0.4 x 0.6 x 3.0 mm, (B) Same scan processed with SwiftMR. Significant noise reduction can be seen across the image, with noticeable differences in the proximal side of the femur and distal part of the tibia. Conspicuity of pathology has also increased with SwiftMR processing.

and accelerated input images, although the margins were relatively smaller. Statistical significance in favor of SwiftMR™-processed exams was seen across all evaluation categories when compared with the SOC. Scores are summarized in Table 4.

SwiftMR™'s clinical implications

The results illustrated above demonstrate that SwiftMR™ can be applied to a wide variety of clinical scenarios spanning the full range of radiology subspecialties, scanner hardware, and imaging sequences. This study included a diverse set of images from neuro, musculoskeletal, and body imaging sections, including images confirmed without (43%) and with (57%) pathologies. Hardware-related factors such as vendor (GE: 17%, Philips: 29%, Siemens: 42%, and Esaote: 12%) and field strength (0.25T: 12%, 1.5T: 44%, 3T: 44%) were also considered to ensure a rigorous validation study. The 18 board-certified radiologists who participated in the study showed consistent responses in support of SwiftMR™ as a superior choice for higher image quality and diagnostic value.

One major benefit of enhancing DICOM image quality during post-processing is the potential for scan time reduction. Several published works(10–12), have shown that SwiftMR™ can add value even to tertiary hospital institutions, addressing the pressing need for optimized protocols and diagnostic accuracy across a broad range of clinical scenarios. These studies showed that even though additional acceleration was achieved on top of the institutional standard-of-care, SwiftMR™-processed images displayed non-inferior or even superior image quality and diagnostic value. Most of these studies also utilized multiple scanners from different vendors

Table 4 - Averaged scores for body imaging subgroups.

	Accelerated	SOC	SwiftMR™ -processed	p-value*	p-value†
Anatomical Conspicuity	3.93	3.90	4.16	< 0.05	< 0.05
Lesion Conspicuity	3.30	3.18	3.72	< 0.05	< 0.05
Subjective SNR	3.87	3.92	4.22	< 0.05	< 0.05
Subjective Resolution	3.86	3.81	4.11	< 0.05	< 0.05
Subjective Contrast	4.04	4.01	4.24	= 0.07	< 0.05

*p-value comparing accelerated input image and SwiftMR™-processed accelerated image, †p-value comparing standard-of-care image and SwiftMR™-processed accelerated image.

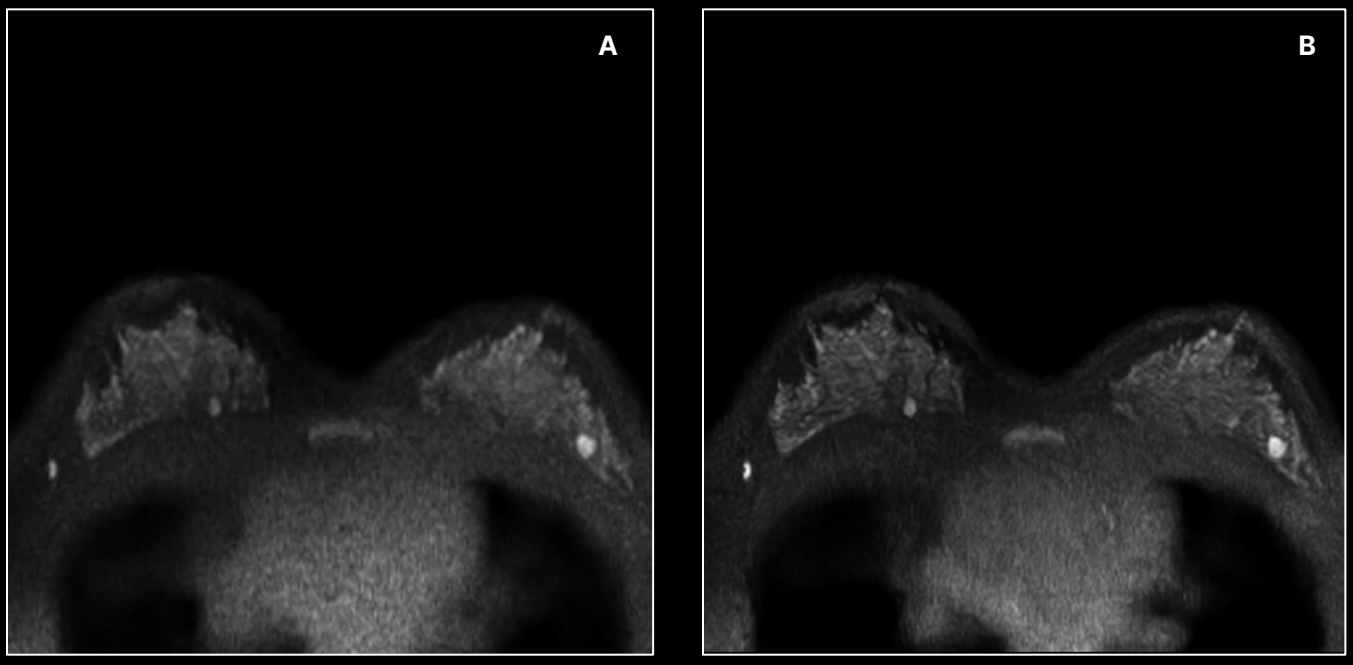

Figure 13 - Denoising and resolution enhancement example for 2D diffusion-weighted breast imaging. (A) SOC image at 1.3 x 1.3 x 3.0 mm, (B) 28% accelerated image processed with SwiftMR, with same acquisition voxel size. Spatial resolution has noticeably increased with SwiftMR.

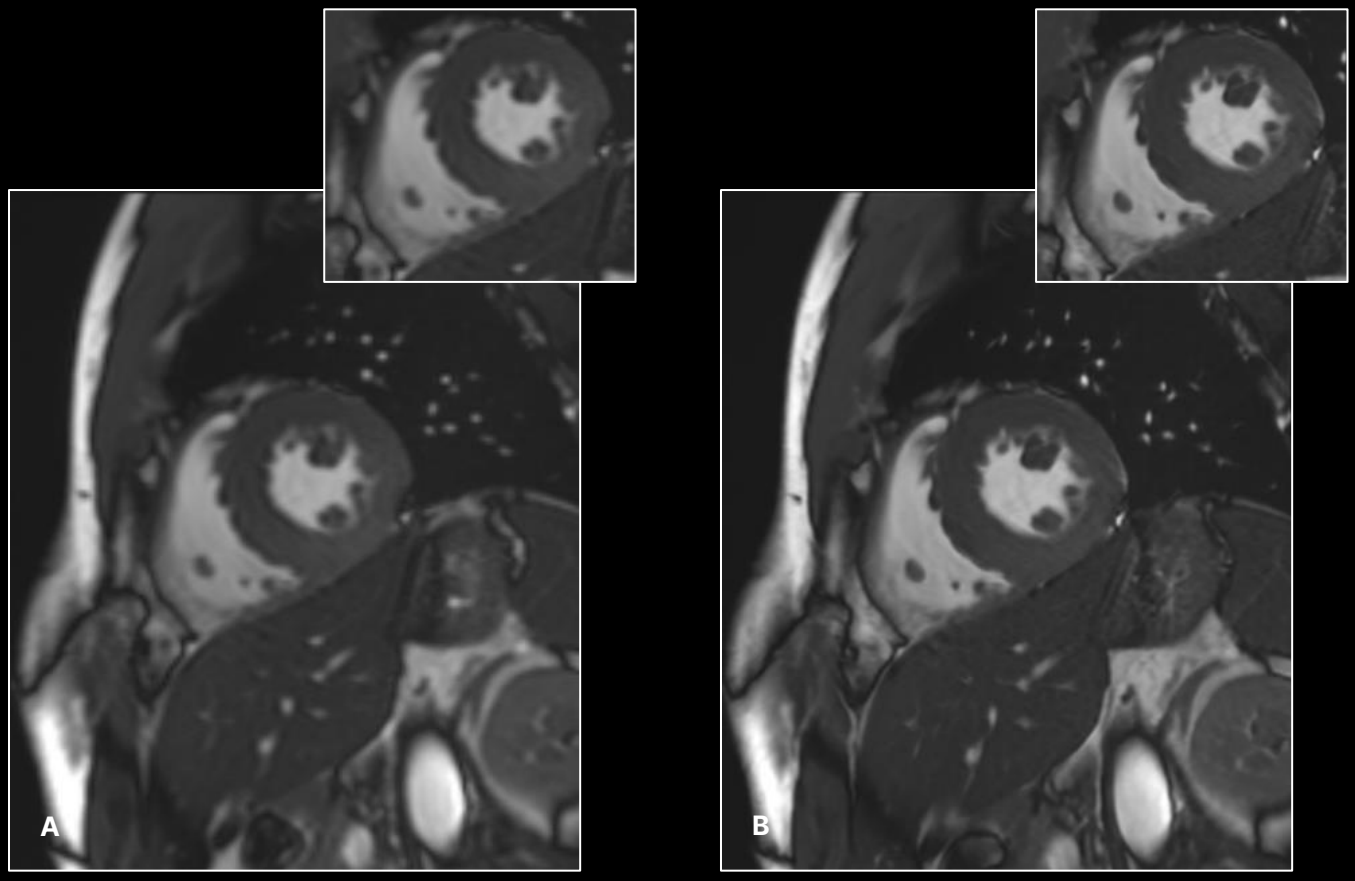

Figure 14. Cardiac cine imaging example with 2D TRUFI. (A) SOC image at 1.4 x 2.2 x 6.0 mm, (B) 38% accelerated image processed with SwiftMR, with 1.4 x 1.8 x 6.0 mm. Scan time reduction was achieved despite smaller acquisition voxel sizes, along with shorter breath-hold time for the patient. Spatial resolution has noticeably increased with SwiftMR.

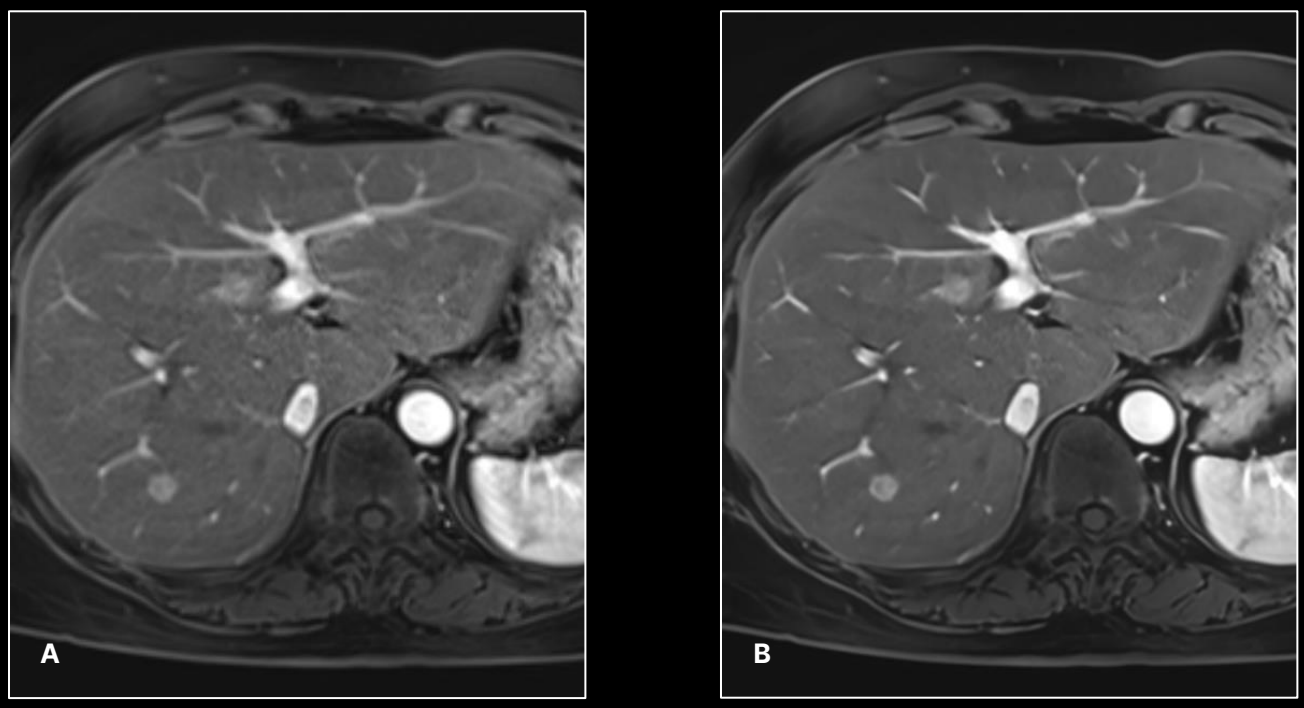

Figure 15. Example of arterial phase dynamic contrast enhanced MRI of the liver. (A) SOC image at 1.0 x 1.4 x 6.0 mm, (B) Same image processed with SwiftMR. Noticeable reduction in noise and resolution enhancement can be seen after SwiftMR processing

to fully demonstrate the vendor-agnostic capabilities of SwiftMR™, which is shown to accommodate different noise characteristics arising from diverse signal acquisition methods and image post-processing methods unique to each scanner system.

Another beneficial aspect of scan acceleration is increased patient comfort. This has well-known, direct implications for claustrophobic patients, patients with difficulty cooperating, and pediatric patients who require sedated exams. The reduction in time spent in the scanner complements technological advancements that enable free-breathing or single breath-hold exams that have become extremely relevant due to the increasing use of MR in body imaging and the subsequent emphasis on breath-hold exams. SwiftMR™ may contribute to this advance by accelerating the breath-hold acquisition for related applications such as cardiac or liver MR imaging. An example is shown in Figure 16.

SwiftMR™'s super-resolution feature is unique in its ability to enhance both the in-plane resolution and the slice resolution (for 3D acquisitions). Traditional k-space-based interpolation applied post-acquisition is aimed to reduce voxel spacing only and does not affect voxel size. Increasing spatial resolution can only be achieved by reducing the actual voxel size, thereby reducing the partial volume effect observed with more signal averaging with larger voxels. SwiftMR™ is capable of enabling true resolution enhancement via AI-powered super-resolution. This works on top of any inline interpolation applied to the image, yielding superior anatomical and pathology details present in the MR image. Figure 17 illustrates the difference between the "native" image, interpolated image and the SwiftMR™-processed image, along with published studies which explore this aspect in detail (13,14).

SwiftMR™'s super-resolution works similarly for 3D acquisitions. Both in-plane and slice super-resolution can be applied simultaneously to such cases, unlocking the true potential for 3D imaging to present unprecedented detail. An example of this is shown in Figure 18.

Concluding remarks

SwiftMR™ offers clinical benefits to a range of MR imaging scenarios. Along with highly customizable enhancements in image SNR and spatial resolution in both 2D and 3D acquisitions, SwiftMR™ is a unique DICOM-based solution which may be applied to any hardware, software, and image configuration. It provides immense advantages over conventional imaging by enabling scan time reduction and image quality enhancement simultaneously, providing value for all stakeholders including healthcare providers, operational managers, and patients. As illustrated above, through an extensive validation process, SwiftMR™ has demonstrated that such disruptive technology is diagnostically relevant and robust, able to strike the balance between scan time and image quality.

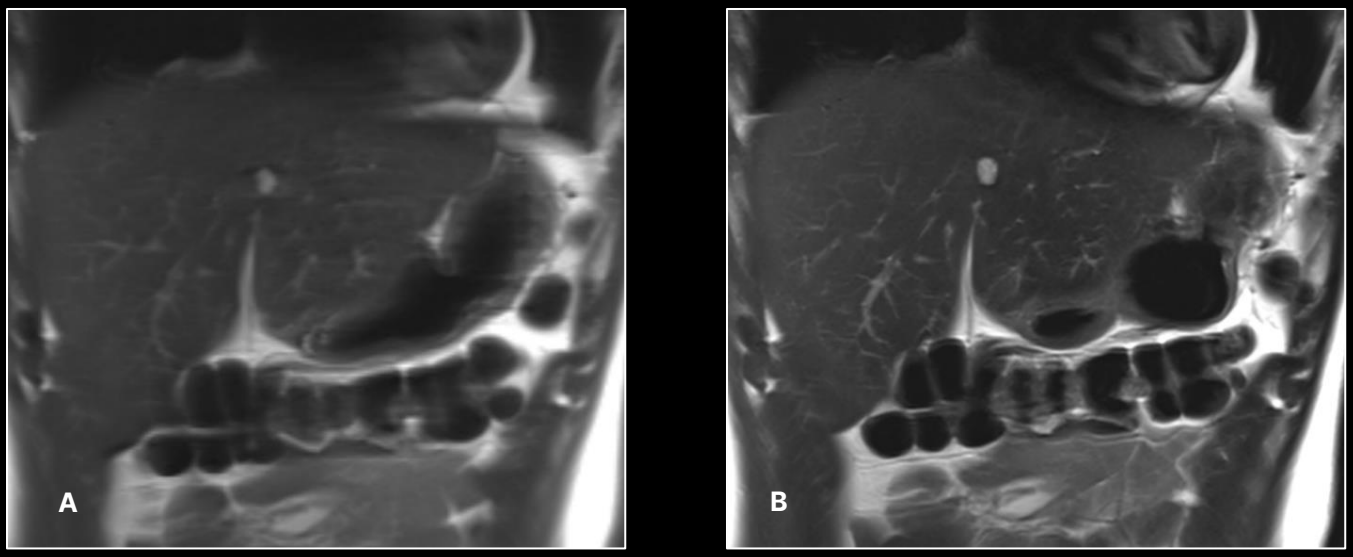

Figure 16 - Comparison of (A) SOC two breath-hold T2-weight liver image at 1.2 x 1.5 x 5.0mm acquired in 33 seconds and (B) single breath-hold image at 1.0 x 1.2 x 5.0 mm acquired in 17 seconds. Significantly improved image quality could be seen with faster, single breath-hold acquisition combined with SwiftMR.

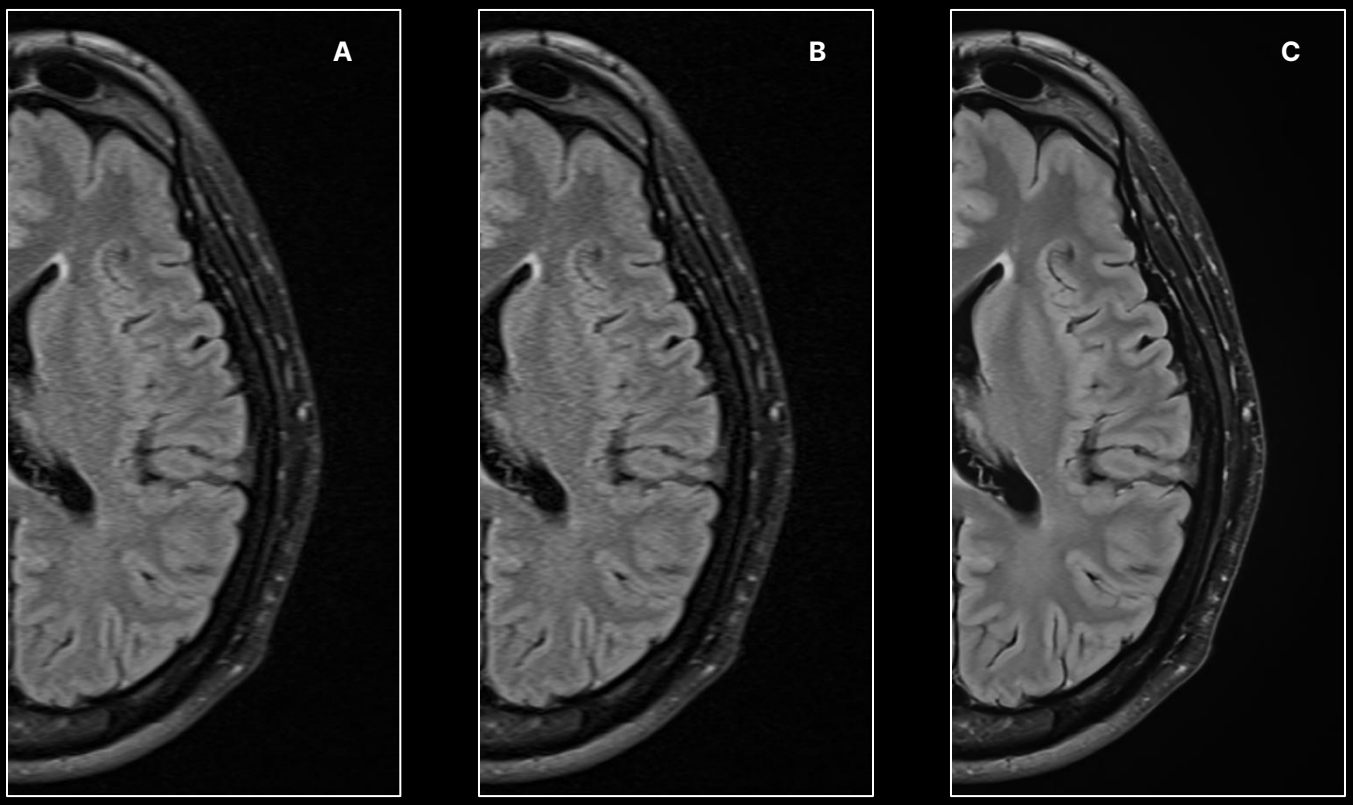

Figure 17. An example illustrating the difference between conventional interpolation and SwiftMR-powered super-resolution. (A) Input “native” image, (B) image with x1.7 interpolation applied, and (C) Input image processed with SwiftMR. Notice superior spatial resolution shown in SwiftMR-processed image, especially for the delineation of the sulci and vasculatures.

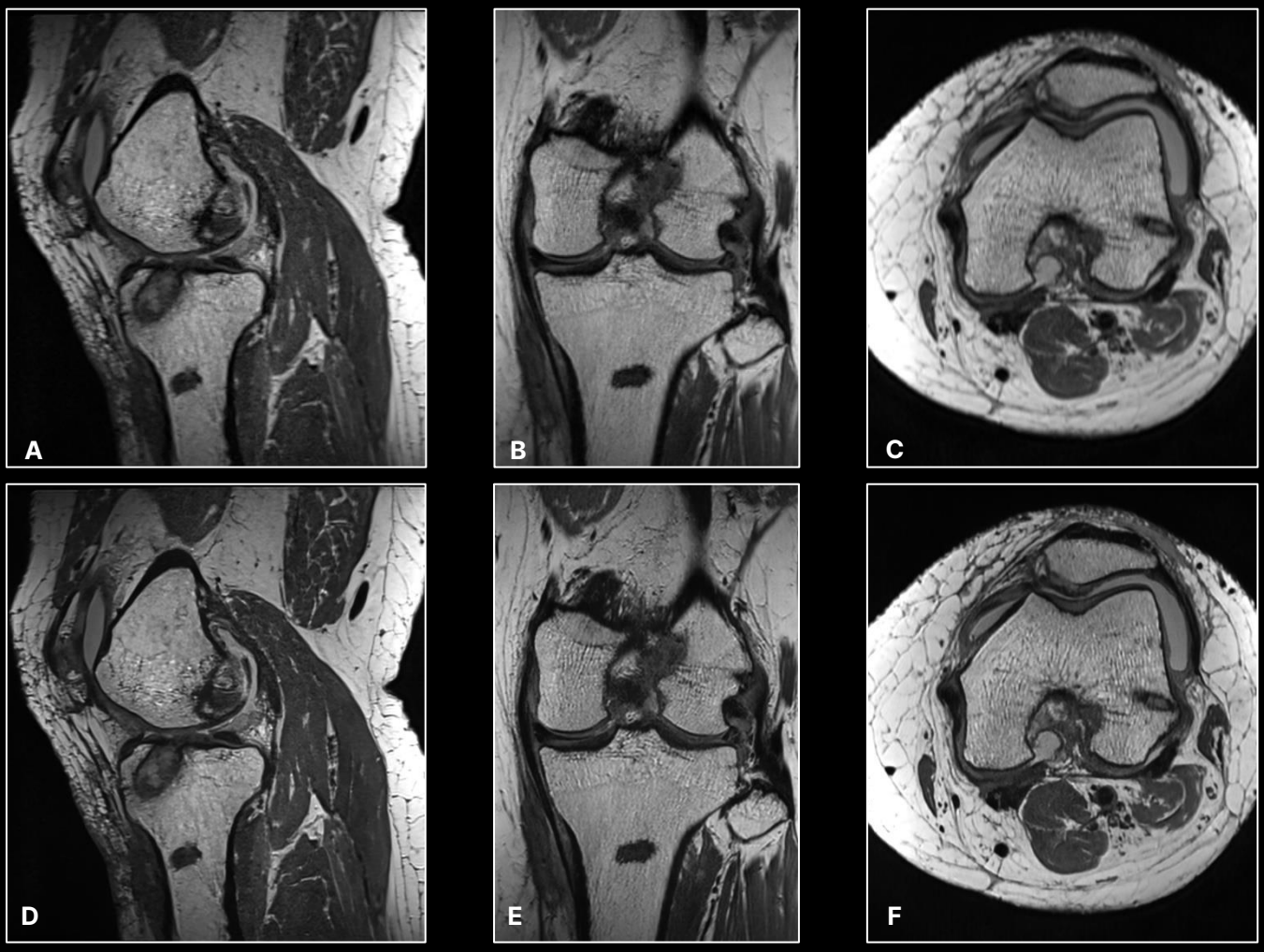

Figure 18. An illustration of improved multi-planar reformat (MPR) with SwiftMR. (A) SOC sagittal T2-weighted source image of the knee, (B) Coronal reformat, and (C) Axial reformat. (D) SwiftMR-processed source image, (E) Coronal reformat, and (F) Axial reformat image. Anatomical conspicuity shown in the reformat images shown in (E) and (F) are higher than that of (B) and (C)

Limitations & disclaimers

The findings we have detailed above were based on real-world data from a limited number of institutions and radiologists. Individual results may vary depending on the standard of care of the institution considering the adoption of SwiftMR™.

References

1. Lacson R, Pianykh O, Hartmann S, Johnston H, Daye D, Flores E, et al. Factors associated with timeliness and equity of access to outpatient MRI examinations. J Am Coll Radiol [Internet]. 2024 Jan 10; Available from: http://dx.doi.org/10.1016/j.jacr.2023.12.028
2. Daye D, Carrodeguas E, Glover M 4th, Guerrier CE, Harvey HB, Flores EJ. Impact of delayed time to advanced imaging on missed appointments across different demographic and socioeconomic factors. J Am Coll Radiol. 2018 May;15(5):713–20.
3. Holbrook A, Glenn H Jr, Mahmood R, Cai Q, Kang J, Duszak R Jr. Shorter perceived outpatient MRI wait times associated with higher patient satisfaction. J Am Coll Radiol. 2016 May;13(5):505–9.
4. Loving VA, Ellis RL, Rippee R, Steele JR, Schomer DF, Shoemaker S. Time is not on our side: How radiology practices should manage customer queues. J Am Coll Radiol. 2017 Nov;14(11):1481–8.
5. Parikh P, Klanderman M, Teck A, Kunzelman J, Banerjee I, DeYoung D, et al. Effects of patient demographics and examination factors on patient experience in outpatient MRI appointments. J Am Coll Radiol. 2024 Apr;21(4):601–8.
6. Dantendorfer K, Amering M, Bankier A, Helbich T, Prayer D, Youssefzadeh S, et al. A study of the effects of patient anxiety, perceptions and equipment on motion artifacts in magnetic resonance imaging. Magn Reson Imaging. 1997;15(3):301–6.
7. MacKenzie R, Sims C, Owens RG, Dixon AK. Patients' perceptions of magnetic resonance imaging. Clin Radiol. 1995 Mar;50(3):137–43.
8. Alvarez IN, Madl J, Becker L, Amft O. Patients' experience to MRI examinations-A systematic qualitative review with meta-synthesis. J Magn Reson Imaging [Internet]. 2024 Mar 27; Available from: http://dx.doi.org/10.1002/jmri.29365
9. Jeong G, Kim H, Yang J, Jang K, Kim J. All-in-one deep learning framework for MR image reconstruction [Internet]. arXiv [eess.IV]. 2024. Available from: http://arxiv.org/abs/2405.03684
10. Yoo H, Yoo R-E, Choi SH, Hwang I, Lee JY, Seo JY, et al. Deep learning-based reconstruction for acceleration of lumbar spine MRI: a prospective comparison with standard MRI. Eur Radiol. 2023 Dec;33(12):8656–68.
11. Lee J, Jung M, Park J, Kim S, Im Y, Lee N, et al. Highly accelerated knee magnetic resonance imaging using deep neural network (DNN)-based reconstruction: prospective, multi-reader, multi-vendor study. Sci Rep. 2023 Oct 12;13(1):17264.
12. Choi KS, Lee JY, Lee KH, Jeon YH, Park C, Jung W, et al. Prospective Validation of Accelerated Brain MRI Using Deep Learning-Based Reconstruction: Simultaneous Application to Spin-Echo and Gradient-Echo Sequences. In: Proceedings of the RSNA 2023. 109th Annual Meeting of the Radiological Society of North America; (2023-SP-9711-RSNA).
13. Suh PS, Park JE, Roh YH, Kim S, Jung M, Koo YS, et al. Improving diagnostic performance of MRI for temporal lobe epilepsy with deep learning-based image reconstruction in patients with suspected focal epilepsy. Korean J Radiol. 2024 Apr;25(4):374–83.
14. Lee SW, Yang S, Kim J. High-Resolution Bone Image from shoulder MRI Using Deep Neural Network on 3-D Accelerated Dixon GRE (CAIPIRINHA Dixon). In: Proceedings of the RSNA 2023. 109th Annual Meeting of the Radiological Society of North America; (2023)-SP-13998-RSNA).

contact@airsmed.com
T: +1 847-306-8731
airsmed.com/en

Chicago Office
475 North Martingale Rd. Suite 710
Schaumburg, IL 60173

AIRS MEDICAL